Analysis of ocean wave characteristic in Western Indonesian Seas using wave spectrum model

Rima Rachmayani[1], *Nining Sari* Ningsih[1], *Hani* Ramadhan[1], *Suliskania* Nurfitri[1]

[1]Department of Oceanography, Faculty of Earth Science and Technology, Bandung Institute of Technology, Indonesia

Abstract. Understanding the characteristics of the ocean wave in Indonesian Seas particularly in western Indonesian Seas is crucial to establish secured marine activities in addition to construct well-built marine infrastructures. Three-years-data (July 1996 - 1999) simulated from Simulating Waves Nearshore (SWAN) model were used to analyze the ocean wave characteristics and variabilities in eastern Indian Ocean, Java Sea, and South China Sea. The interannual or seasonal variability of the significant wave height is affected by the alteration of wind speed and direction. Interactions between Indian Ocean Dipole Mode (IODM), El Niño Southern Oscillation (ENSO) and monsoon result in interannual ocean wave variability in the study areas. Empirical Orthogonal Functions (EOF) analysis produces 6 modes represents 95% of total variance that influence the wave height variability in the entire model domain. Mode 1 was dominated by annual monsoon and has spatial dominant contribution in South China Sea effected by ENSO and Indian Ocean influenced by IODM. Java Sea was influenced by Mode 2 which is controlled by semi-annual monsoon and IODM. A positive (negative) IODM strengthens (weakens) the winds speed in Java Sea during the East (West) season and hence contributes to Mode 2 in increasing (decreasing) the significant wave in Java Sea.

1 Introduction

Various activities on seas, either for sea transportation activities, fisheries, marine resources exploration, and also development in marine sector are very sensitive to weather and sea condition changes. Two hundred sixty cases of ship accidents were due to natural factor increased with years [1]. Among various natural factors, one that greatly influences marine activities is wave, and therefore, in the marine meteorological services, in addition to wind information, wave information is the most important part that should exist in every kind of marine weather information [1]. The existence of extreme high tides could threaten the safety on sea and may result in great losses.

The wave conditions in the waters are strongly influenced by wind variability as the dominant force of ocean waves [2]. Indonesia is an area affected by the monsoon wind cycle. The monsoon interacts with an interannual phenomenon such as El Niño-Southern Oscillation (ENSO) and Indian Ocean Dipole Mode (IODM); affects regional and local wind circulation patterns in Indonesian waters [3]. Characteristics of waves and the influence of interannual phenomenon such as ENSO and IODM to wave variability in the waters can be determined from long-term wave measurements. Some sources of data buoy measurement, Voluntary Observing Ship (VOS), and altimeter satellite measurement can be utilized as a basis for determining wave climate. In addition, the wave hindcasting data using model is also can be used as an alternative data.

Characteristics and variability of waves in the waters of western Indonesia, including the South China Sea, Indian Ocean, and Java Sea are addressed in this study. The wind field in the mentioned three waters is strongly influenced by the relative position of the sun against the earth and it is influenced by the IODM system. This study addresses two main issues: (1) how the dominant variability pattern can influence the variability of the wave, (2) how it interacts with the interannual phenomenon of ENSO and IODM. This paper is organized as follows: the study area is introduced in Sect. 2, and the details of data used and the methodology are presented in Sect. 3. Section 4 presents the results and discussion of the study, and the conclusions are given in Sect. 5.

2 Study area

This study focusses on the territorial waters of western Indonesia between 20°N – 23°S and 95°E – 120°E. The boundary covers the eastern Indian Ocean, South China Sea, and Java Sea. Domains are further extended towards the Indian Ocean to accommodate the perfect wave formation state in the region. Figure 1 shows the model domains and bathymetry profiles. The study area is strongly influenced by the monsoon wind. There is a trough in southern Java and Sumatra marked by a very steep bathymetry changes. Meanwhile, the Java Sea is a shallow sea with a depth ranging from 50 m. The northern part of the South China Sea reaches a depth of about 4500

* Corresponding author: rrachmayani@oceanography.itb.ac.id

© The Authors, published by EDP Sciences. This is an open access article distributed under the terms of the Creative Commons Attribution License 4.0 (http://creativecommons.org/licenses/by/4.0/).

m while the southern part is around 100 m. Seamount in the South China Sea can cause a significant wave energy reduction either through the process of dissipation due to basic friction and dissipation due to breaking waves.

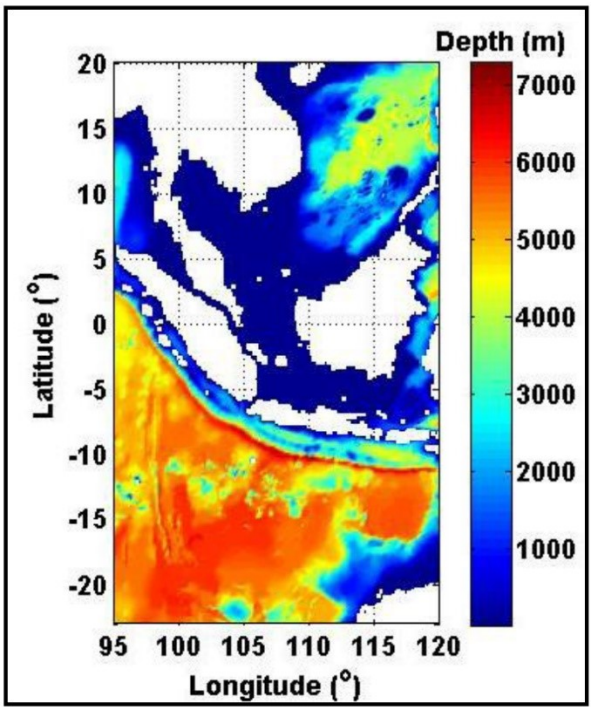

Fig. 1. Domain model and bathymetry profiles

3 Methodology

3.1. Data

In this study, wind and bathymetry data are applied as model input. The wind field is taken from 10 m above sea level called CCMP (Cross Calibrated Multi Purposed) with a gradient resolution of 0.25° x 0.25° and intervals every 6 hours. Meanwhile, bathymetry data from GEBCO (Global Bathymetric Chart of Oceans) produced with 1' x 1' resolution [4]. The influence of tides and changes in depth due to sedimentation is negligible, so the depth value is considered constant during the hindcasting period (July 1996 - 1999).

3.2 Model

Simulating Wave Nearshore (SWAN) is a third-generation wave model for obtaining realistic estimates of wave parameters in coastal areas, lakes and estuaries from given wind, bottom and current conditions. However, SWAN can be used on any scale relevant for wind-generated surface gravity waves. The model is based on the wave action balance equation with sources and sinks [5, 6].

In this study, hindcasting wave was performed by using model of SWAN with nonstationary mode where the input of wind field always change every step of time. The physical processes activated in this simulation are development of wind wave, quadruplet nonlinear interaction, dissipation due to white-capping, basic friction, and breaking waves. In this study, the initial spectrum used in the model is the initial spectrum of Joint North Sea Wave Project (JONSWAP). Meanwhile, the discrete wave propagation in the geographic space uses the BSBT (backward in space and backward in time) scheme. The formulation of the wind source/development of wind wave and white-capping function employed in the model is described in [7, 8] and the basic friction function performed in the study followed the formulation in [8, 9]. Here are the SWAN model configurations applied to this study:

Resolution	:	1/6° x 1/6°
Frequency	:	Frequency with lowest frequency 0.04 Hz and highest 1 Hz
Space- θ	:	180 mesh in-space θ for a full circle 360°
Domain	:	20°N – 23°S and 95°E – 120°E with resolution 1/6° x 1/6°

The model runs for 3 years (July 1, 1996, 00 00 UTC to June 30, 1999, 18 00 UTC), with a spin-up period (from calm state) for the first 7 days. Model output is the significant wave height and direction of propagation.

3.2. Emphirical Ortogonal Function

Empirical Orthogonal Function (EOFs) technique aims at finding a new set of variables that capture most of the observed variance from the data through a linear combination of the original variables. EOFs have been introduced in atmospheric science since the early 50's [10, 11]. EOF techniques are deeply rooted in statistics and EOFs was introduced as principal component analysis (PCA) [12] and it is analyzed details [13, 14].

To obtain the main patterns of wave fields variability in this current study, EOFs was performed in determining the variation of significant wave height (H_s) values in the model domain either temporally or spatially. The time series of the EOFs principal components (PCs) are normalized to have unit variance, so that the corresponding EOFs represent the typical variability of the data in their original units.

4 Results and Discussion

4.1 Wind and Significant Waves Height (H_s)

The model results show a linier relationship between the higher of wind speed and the higher of H_s. The direction of wave propagation is strongly influenced by the wind direction. Waves generally move in the direction of the wind, except in areas with considerable refraction effects such as waters near the coast. The seafloor indicated by significant depth as found in the South China Sea (SCS) causes significant wave heights in the area to be relatively smaller as the wave energy is dissipated by increasingly larger friction and steep bathymetry changes can cause breaks.

The significant wind direction and wave height of the model in the west season (DJF) is shown in Figure 2. The significant monthly wind and wave height is the result of

the reduction of the wind and H_s for each month for 3 years. The x and y direction components of the wind field and H_s are averaged separately to determine the mean direction of wind movement and significant wave propagation. In December, maximum winds are located at South China Seas (latitude 10°N - 20°N) and in January and February months winds in the South China Seas weaken. The direction of wave propagation is also in accordance with the direction of the wind. In narrow and closed waters, H_s tends to be relatively lower than H_s in wide and open waters, as large and open waters support perfect waveforms and the inclusion of wave energy from other places through wave propagation phenomena.

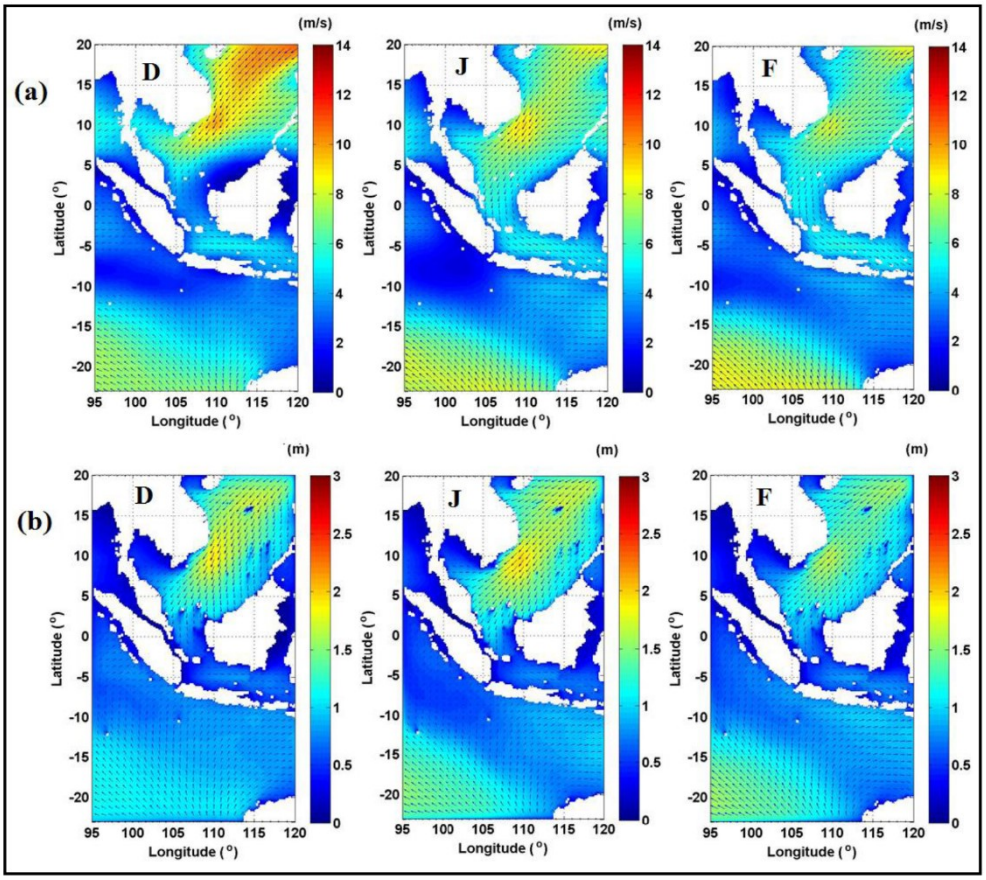

Fig. 2. Averaged of (a) the wind field (m/s) and (b) the significant wave height (m) in December-January-February (DJF)

Meanwhile, the wind field and H_s in the east season (JJA) are shown in Figure 3. During east season (JJA), the winds in South China Sea strengthen again and move toward northeast. Similarly, the winds in Java Sea (JS) also increase and move from the east and reach its maximum in August. The wave simulation results show the similar seasonal pattern with the wind field. Moreover, during JJA the wind field increases strongly in Indian Ocean (IO) between 10°S – 20°S. In general, the wind field in Indian Ocean near the equator is smaller than any other place in Indian Ocean. However, the Hs in Indian Ocean near the equator is a result of traveled wave energy from other regions in Indian Ocean.

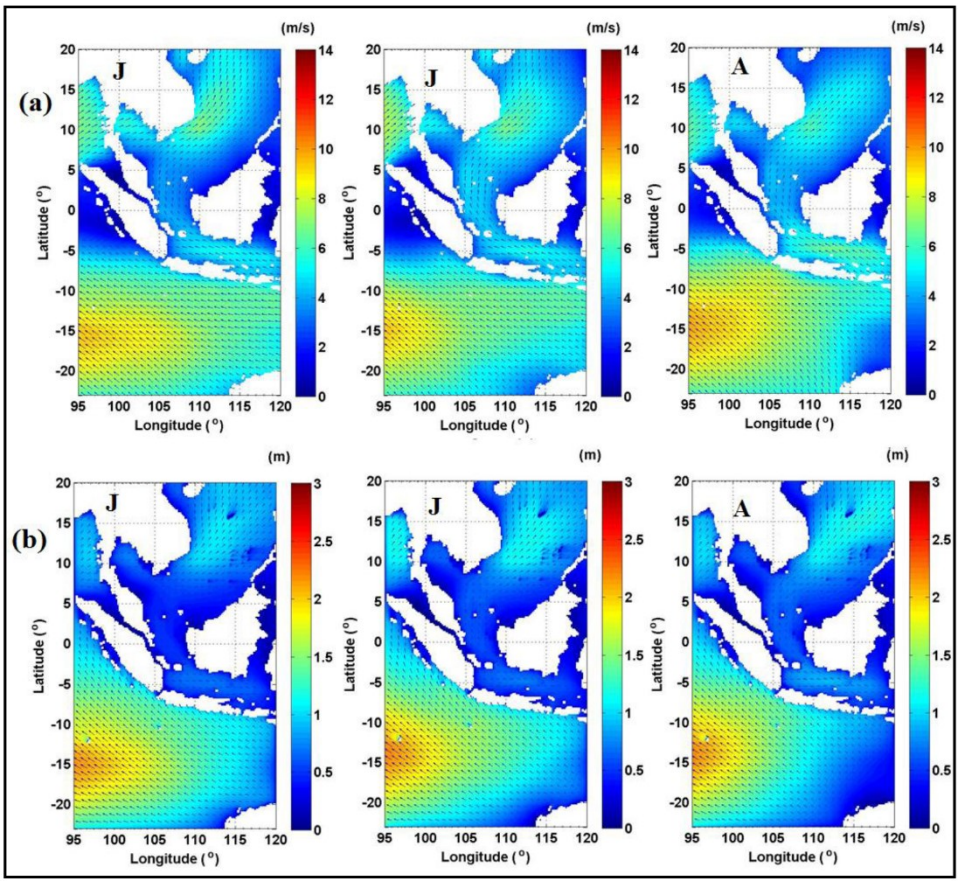

Fig. 3. As in Fig. 2 but for June-July-August (JJA)

4.2 Results of EOF Analysis

The result of significant wave height simulation affirms significant variation of H_s to time at the three waters. Figure 4 shows the mean significant wave heights in the model domains. The highest average H_s up to 1.75 m is in Indian Ocean, followed by South China Sea up to 1.3 m. The average H_s value in Java Sea is lower than 1 m, smaller than in South China Sea and Indian Ocean due to a narrower and closed water in Java Sea. Moreover, wind speed passing through Java Sea is not as big as in South China Sea and Indian Ocean.

The EOF analysis in this study uses the monthly average of H_s value and yields 6 modes representing 95% of the total variance as shown in Figure 5. Mode 1 represents 52.97%, Mode 2 represents 27.02%, and Mode 3 to Mode 6 represents only 15.10% of the total variance. Significant wave height variability in the model domains is dominated by the effects of Mode 1 and Mode 2. EOF analysis accommodates temporal/amplitude patterns of modes.

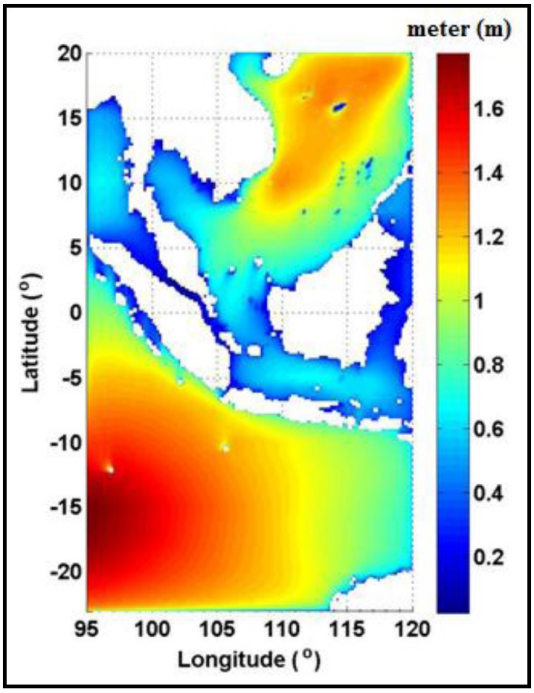

Fig. 4. Mean significant wave heights over 36 months (m)

* Corresponding author: rrachmayani@oceanography.itb.ac.id

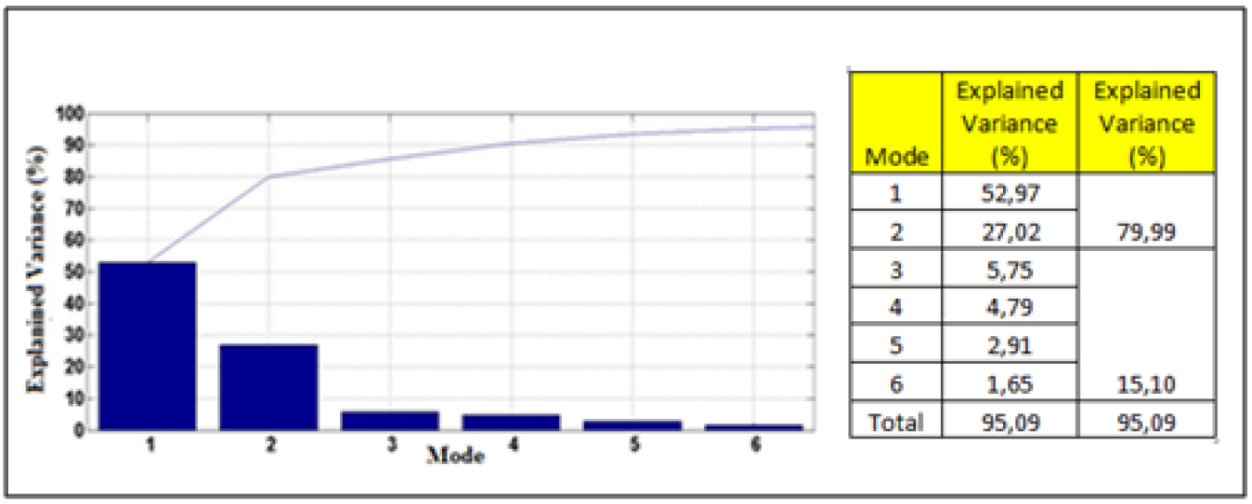

Mode	Explained Variance (%)	Explained Variance (%)
1	52,97	
2	27,02	79,99
3	5,75	
4	4,79	
5	2,91	
6	1,65	15,10
Total	95,09	95,09

Fig. 5. Six modes represents of 95% total variance

The spatial pattern of Mode 1 is exhibited in Figure 6a. South China Sea is dominated by two positive poles located at latitude 10°N – 17°N. The position of the two poles coincide with the maximum wind in the South China Sea during the west season (DJF). Meanwhile, Indian Ocean is controlled by a negative spatial pattern around latitude 12°S. This indicates a reversed temporal variability phase between South China Sea and Indian. Temporal pattern of Mode 1 is displayed in Figure 6c. In general, the high (low)-peak temporal pattern of Mode 1 occurs in the west (east) season. During west (east) season, South China Sea experiences a higher (lower) H_s and Indian Ocean captures a lower (higher) H_s value than its average. Temporal patterns Mode 1 is a composite of various signals with different periods. To find out the various signals, a power spectrum analysis is performed on the temporal pattern of Mode 1. The result of power spectrum analysis for the six PCs is affirmed in Figure 7. Annual monsoon plays a role in Mode 1 (Figure 7a).

* Corresponding author: rrachmayani@oceanography.itb.ac.id

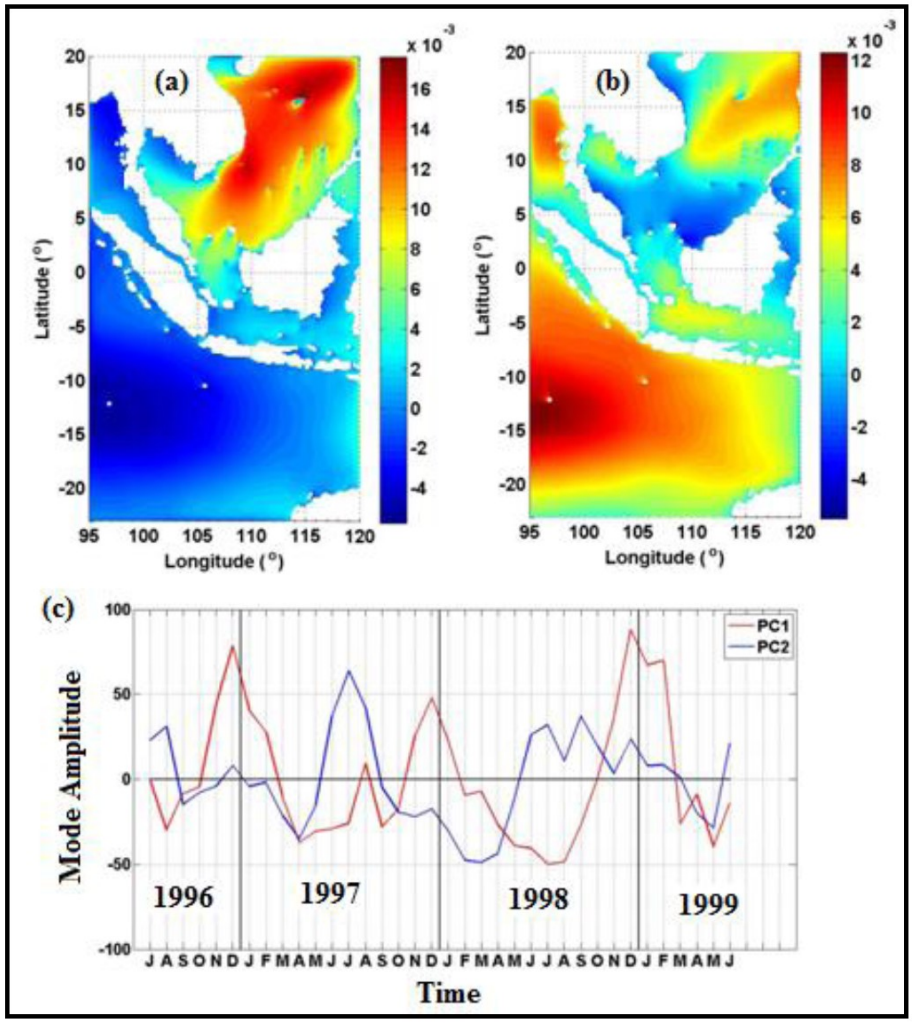

Figure 6. EOF analysis results: (a) Spatial pattern of Mode 1, (b) Spatial pattern of Mode 2, and (c) mode amplitude/temporal pattern of Mode 1 and Mode 2

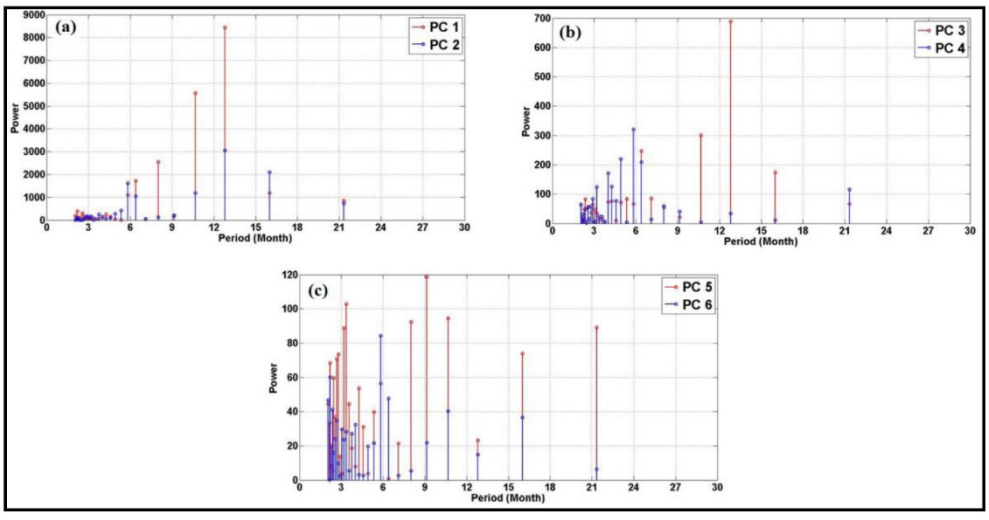

Fig. 7. The spectrum energy of mode amplitude/temporal pattern: (a) Mode 1 and Mode 2, (b) Mode 3 and Mode 4, and (c) Mode 4 and Mode 5

* Corresponding author: rrachmayani@oceanography.itb.ac.id

Spatial pattern of Mode 2 is presented in Figure 6b. Almost all domains have a positive spatial pattern. This shows a similar phase of variability with the maximum value in Indian Ocean. The value of spatial patterns in Java Sea and Atlantic Ocean (AO) is quite large; indicates the huge effect of Mode 2 in both waters. Meanwhile, some areas in the South China Sea respond as negative and positive spatial pattern values; indicates differences phase variability by Mode 2 in South China Sea. Temporal pattern/mode amplitude of Mode 2 is exposed in Figure 6c shows the presence of two peaks in one year (i.e., in the west and east seasons). Spectrum analysis for temporal pattern of Mode 2 is shown in Figure 7. Based on the spectrum analysis, Mode 2 is determined by the semi-annual monsoon.

The spatial patterns of Mode 3 to Mode 6 are respectively displayed in Figures 8 and 9. Mode 3 to Mode 6 contributes only 15% to total variance. Mode 3 illustrates two areas with different spatial pattern in Indian Ocean, as well as in South China Sea. Based on spectrum analysis, Mode 3 is still controlled by 12 monthly signals but modulated with smaller-than-6-months signals. Intraseasonal signals play a role in Mode 4, Mode 5, and Mode 6.

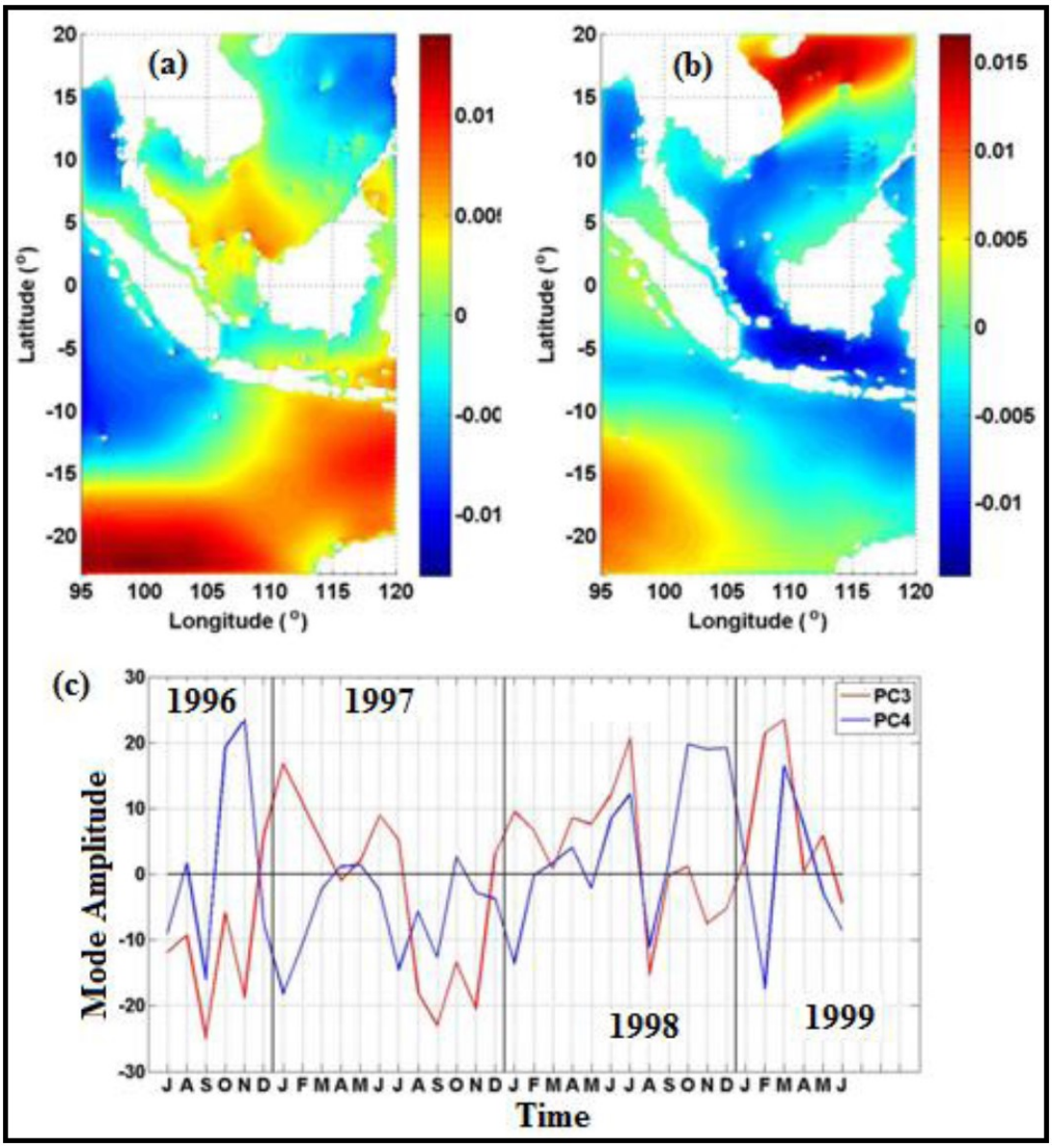

Fig. 8. As in Fig. 6 but for Mode 3 and Mode 4

* Corresponding author: rrachmayani@oceanography.itb.ac.id

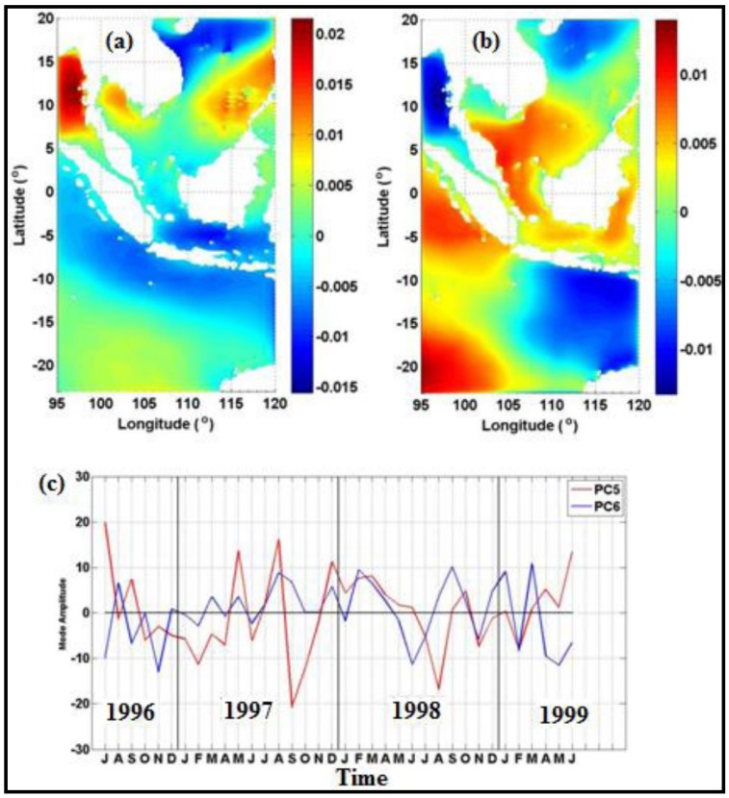

Fig. 9. As in Fig. 6 but for Mode 5 and Mode 6

4.3 Results of EOF Analysis Test

The EOF analysis produces modes that affect significant wave height variability in the model area. The EOF analysis test has been done by comparing the number of multiplication products between the spatial pattern value and the temporal pattern with the input data (not shown). Figure 10 displays the five test points of the EOF analysis results.

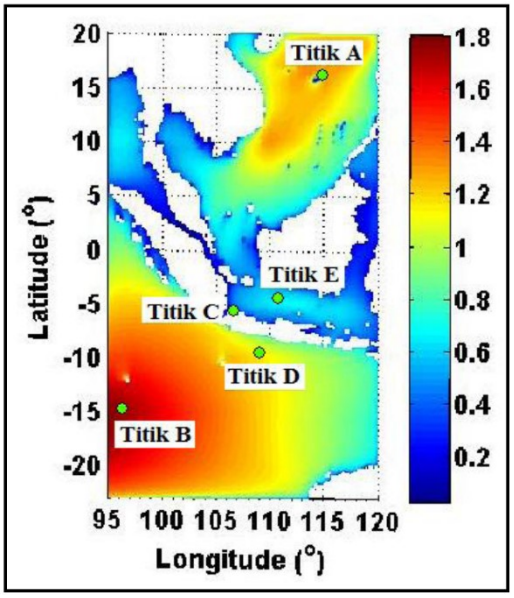

Fig. 10. Five test points of the EOF analysis results

Based on the multiplication of the spatial pattern (u) and the temporal pattern (a) for the six modes as well as the sum of the spatial (u) and temporal (a) at six PCs at point A to point E exhibits that wave variability from Mode 1 to Mode 6 at Point A is strongly dominated by the effect of Mode 1. The wave variability from Mode 1 to Mode 6 at Point B is dominated by the effects of Mode 1 and Mode 2. At Point C, D and E, the effect of Mode 1 is minor, while Mode 2 contributes in influencing wave variability. Mode 1 becomes the most dominant mode of the whole domain in general due to the largest temporal pattern or amplitude mode.

4.4 Seasonal Wind and Significant Wave Height

Furthermore, based on the results of EOF analysis, in this study, domain model can be divided into 6 areas that are considered to have the characteristics of wave variability. The divided area is illustrated in Figure 11. The wind field and the average H_s for each month for 3 years at the six consecutive areas are shown in Figure 12 and Figure 13. The wind moves from the southeast in Area 1 throughout the year. The maximum wind occurs during east season (JJA) with a great average speed ranging from 6.46 m/s to 7.90 m/s. This corresponds to the maximum average value of simulated H_s results. The minimum average H_s in Area 1 occurs during west season with values between 1.17 m to 1.26 m and corresponds to the lowest wind velocity conditions in Area 1. There is a difference in the wind

field pattern between Area 1 and 2. In Area 2, the wind moves from the southwest during west season with an average H_s value of 1.0 m.

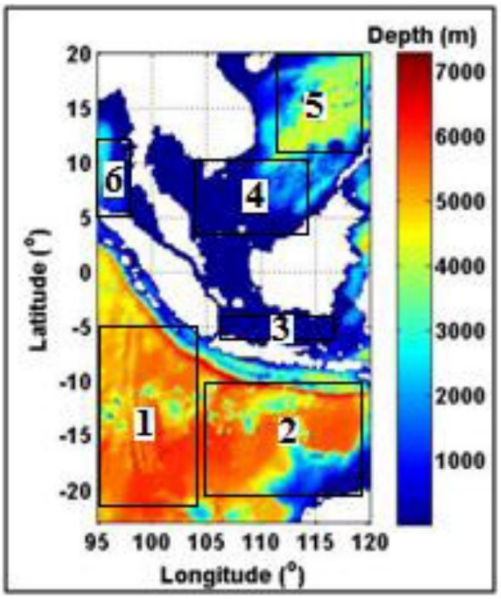

Fig. 11. Six divided area

Maximum waves occur during east season with a range of 1.1 m to 1.4 m. Area 3 represents Java Sea with a wind field pattern that changes direction almost 180° in one year. The wind moves from the southeast with a maximum speed of 4.54 m/s to 5.61 m/s during east season and a wave height of 0.6 m to 0.76 m. In Area 4, the wind moves from the northeast during west season with a significant wave height of 1.20 m to 1.60 m. During east season, the wind moves from the southwest with a significant wave height of 0.57 m to 0.66 m. The maximum wind speed and maximum wave height in Area 5 occurs twice in a year (west and east season).

The wave height is significant up to 1.30 m to 1.90 m during west season, whereas during east season the significant wave height reaches 0.90 m to 1.0 m. In Area 6, the dominant wind moves from the northwest from May to September with a significant wave height of 0.56 m to 0.87 m. During west season, the wind moves from the northeast with a significant wave height of 0.34 m to 0.44 m.

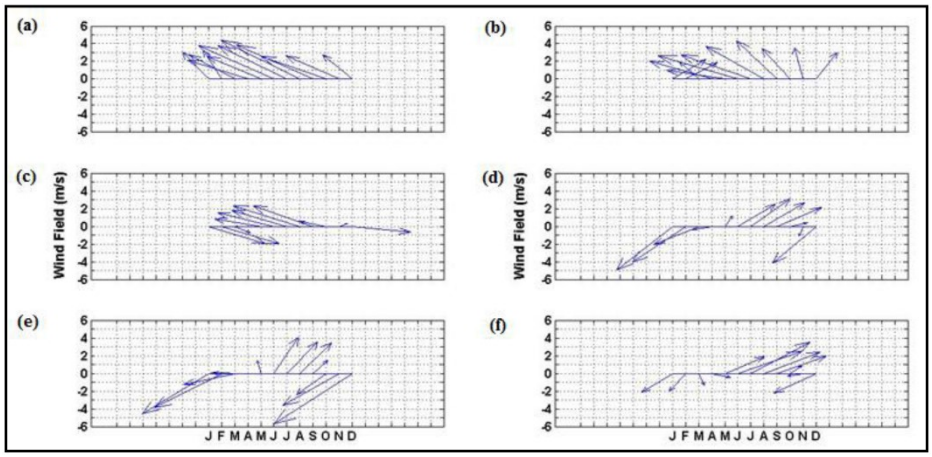

Fig. 12. Average monthly wind field at: (a) Area 1, (b) Area 2, (c) Area 3, (d) Area (4), (e) Area 5, and (f) Area 6

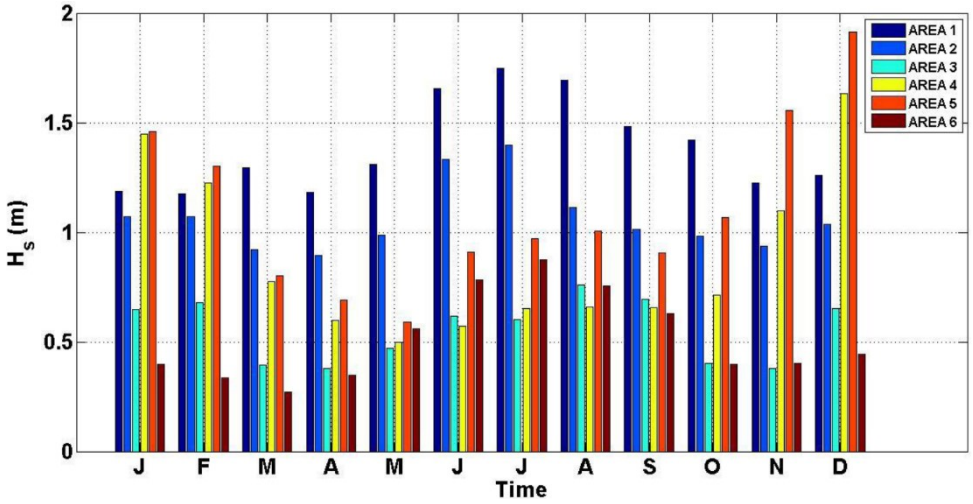

Fig. 13. The averaged significant wave height at all six areas of study

4.5 Analysis of Annual Variations

Based on the results of EOF analysis, it is known that wave variability in domain model is dominantly influenced by Mode 1 and Mode 2. In the previous section also has been explained that a monsoon with a period of 12 months plays a role in Mode 1 and a semi-annual monsoon plays a role in Mode 2. However, there is a discrepancy in the temporal pattern at certain intervals and it is associated with the influence of the interannual phenomenon of IODM and ENSO.

Mode 1 gives the dominant influence in the Indian Ocean and South China Sea with different phase variability. Thus, the analysis was performed separately for both waters and selected a point that has the largest spatial pattern value in the Indian Ocean and South China Sea. In addition, the average monthly wind vector supports the analysis. From Figure 11, point A (South China Sea) and point B (Indian Ocean) are chosen to illustrate interaction between IODM and ENSO to Mode 1 and point E represents Java Sea is picked to capture the interaction of the interannual phenomena to Mode 2.

Figure 14 - 16 expose the plot of Ocean Nino Index (ONI), Dipole Mode Index (DMI), spatial and temporal pattern and the averaged monthly wind field at point A, B, and C, respectively. Interval 1 indicates a normal IODM and ENSO states, index 2 (interval 2) reveals the time interval of positive El-Niño and IODM events, and index 3 (interval 3) affirms the time interval of La-Niña events.

During west season, the mean value of significant wave height at point A ($h_{1,A}$) (South China Sea) at interval 2 is smaller compared at interval 1. This is due to the weakening of monsoon winds during the El-Niño incident. At interval 3, the value of $h_{1,A}$ is greater due to the strengthening of the wind during La Niña event. To conclude, ENSO phenomenon contributes in Mode 1 at point A (South China Sea).

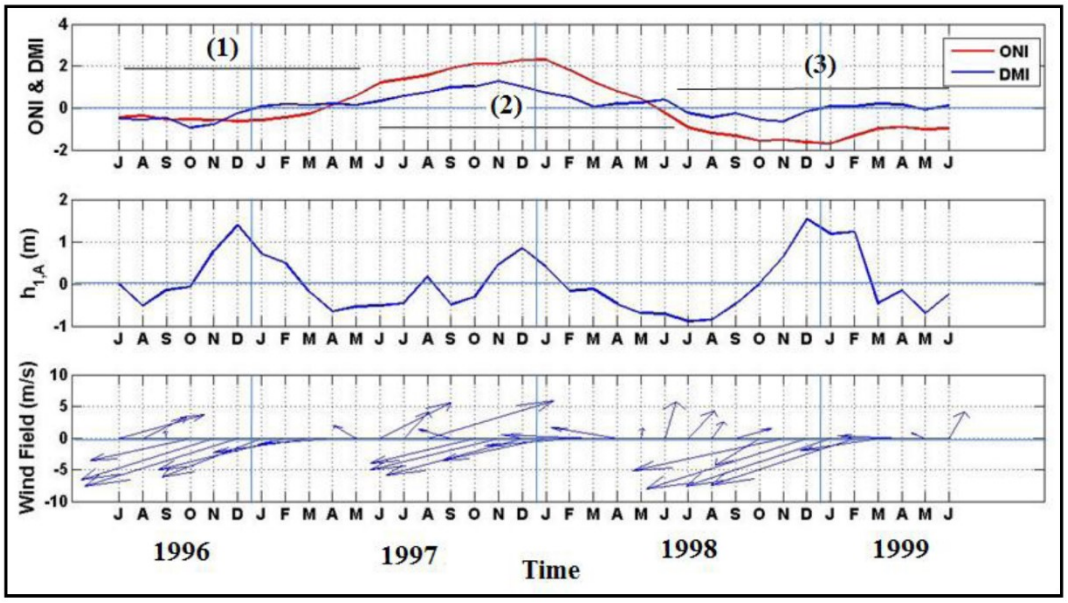

Fig. 14. ONI and DMI (top panel), spatial and temporal pattern (middle panel) and the average monthly wind field (bottom panel) at point A (South China Sea)

The maximum (minimum) wave height occurs during east (west) season at point B in Indian Ocean. This is supported by Mode 1 at interval 2 during west season where Mode 1 has a smaller effect in reducing wave heights in the Indian Ocean than its normal state. Positive IODM at interval 2 makes the winds speed larger and move westward; indicates that the IODM affects Mode 1 in Indian Ocean.

As mentioned above, point E is selected to represent Java Sea where contribution of Mode 2 is dominant in affecting wave variability rather than Mode 1. In July to September (JAS) at interval 2, winds in the Java Sea move westward and it is reinforced by a positive IODM which drive stronger winds westward around Java Sea. Meanwhile, in December to February (DJF) at interval 2, the wave at point E becomes smaller than at interval 1. This is associated with a movement of winds eastward in Java Sea which is reduced by the positive IODM.

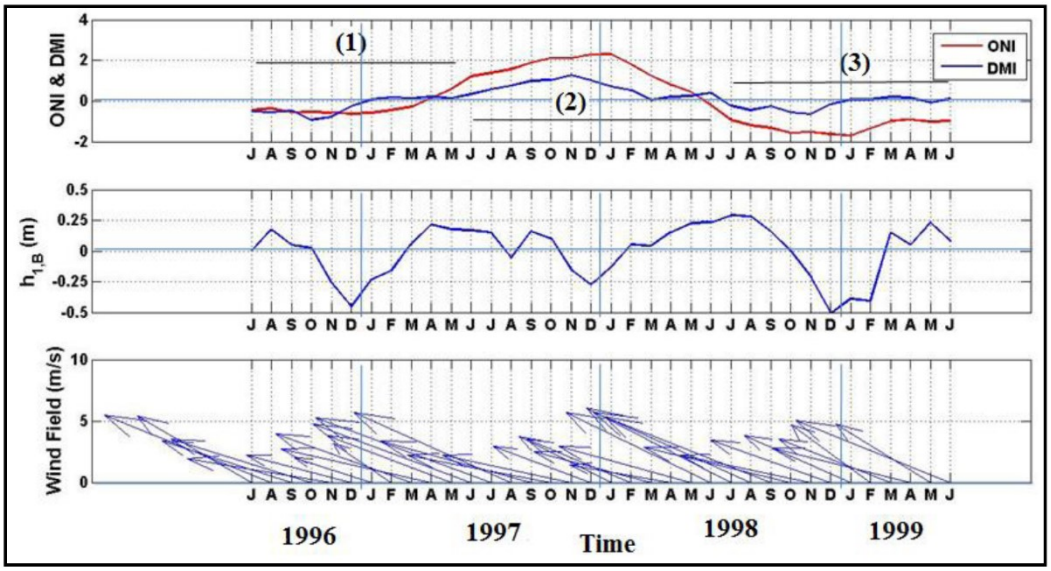

Fig. 15. As in Fig, 14 but for point B (Indian Ocean)

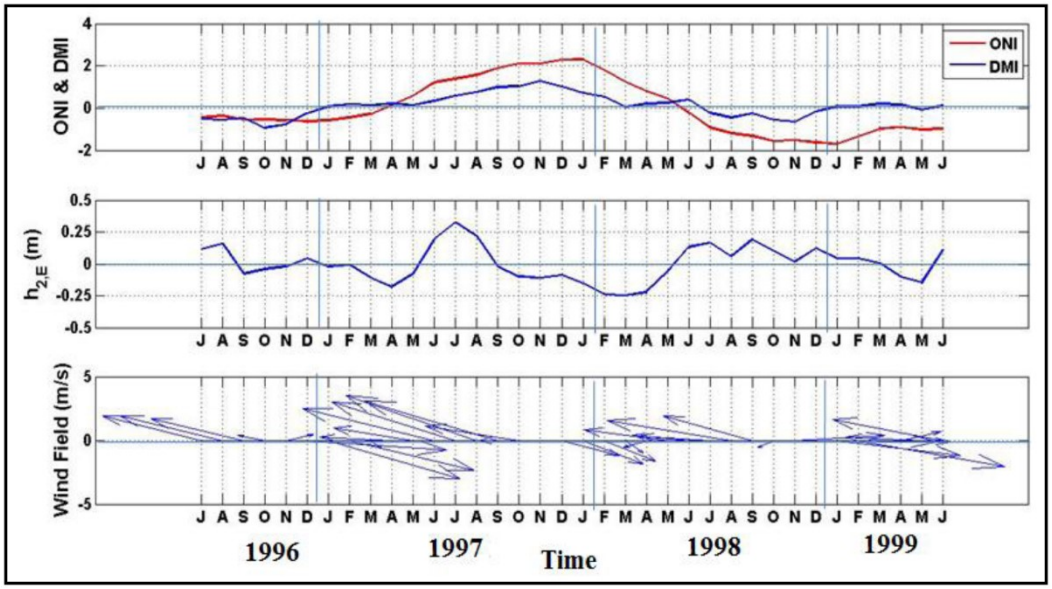

Fig 16. As in Fig, 14 but for point E (Java Sea)

5 Conclusion

Empirical Orthogonal Functions (EOF) analysis produces 6 modes represents 95% of total variance that influence the wave height variability in the entire model domain. Annual monsoon plays a role in Mode and has spatial dominant contribution in South China Sea and Indian Ocean. Java Sea was influenced by Mode 2 which is controlled by semi-annual monsoon. ENSO effect was identified in South China Sea and IODM effect was captured at Indian Ocean in Mode 1 and at Java Sea in Mode 2. A positive (negative) IODM strengthens (weakens) the winds speed in Java Sea during the East (West) season and hence contributes to Mode 2 in increasing (decreasing) the significant wave in Java Sea

References

1. R. Kurniawan and M. K. Khotimah, *Ocean Wave Characteristics in Indonesian Waters for Sea Transportation Safety and Planning*, IPTEK, J. Tech. and Sci., **26**(1), pp. 19-27, (2015).
2. R. A. Arinaga and K. F. Cheung, *Atlas of global wave energy from 10 years of reanalysis and hindcast data*, Renewable Energy, **39**(1), pp. 49-64, (2012).
3. A. Ramdhani, *Variabilitas Iklim Gelombang di Perairan Indonesia (Validasi Model Gelombang Wavewatch III)*, Laporan Kemajuan 1, Program Doktor Sains Kebumian, ITB, Bandung, (2013).
4. IOC, IHO dan BODC, *Centenary Edition of the GEBCO Digital Atlas*, Intergovernmental Oceanographic Commission dan the International Hydrographic Organization sebagai bagian dari General Bathymetric Chart of the Oceans; British Oceanographic Data Centre, Liverpool, (2003).
5. I. R. Young, *Seasonal variability of the global ocean wind and wave climate*, Int. J. Clim., **19**(9), pp. 931 – 950, (1999).
6. N. Booij, N., R. C. Ris, and L.H. Holthuijsen, *A third-generation wave model for coastal regions. Part I: Model description and validation*, J. Geophys. Res., **104**, 7649 – 7666, (1999).
7. G. J. Komen, S. Hasselmann, and K. Hasselmann, *On the existence of a fully developed wind-sea spectrum*, J. Phys. Oceanography, 14, 1271 – 1285, (1984).
8. The SWAN Team, *SWAN Scientific and Technical Documentation*, Delft University of Technology, Netherlands, (2013).
9. O. S. Madsen, Y. -K. Poon, and H. C. Graber, *Spectral wave attenuation by bottom friction: Theory. Proc.*, 21st Coastal Engineering Conf., ASCE, (1988).
10. A. M. Obukhov, *Statistically homogeneous fields on atmosphere*, Usp. Mat. Navk., **2**, pp. 196 – 198, (1947).
11. A. M. Obukhov, *The statistically orthogonal expansion of empirical functions*, Bull. Acad. Sci, USSR Geophys. Ser. (English Transl.), pp. 288 – 291, (1960).
12. H. Hotelling, *Analysis of a complex of statistical variables into principal components*, J. Educ. Psych, **24**, pp. 417 – 520, (1933).
13. D. S. Wilks, *Statistical Methods in the Atmospheric Sciences*, Academic Press, San Diego, (1995).